

Effect of Cyanato, Azido, Carboxylato, and Carbonato Ligands on the Formation of Cobalt(II) Polyoxometalates: Characterization, Magnetic, and Electrochemical Studies of Multinuclear Cobalt Clusters

Laurent Lisnard,^[a] Pierre Mialane,*^[a] Anne Dolbecq,^[a] Jérôme Marrot,^[a] Juan Modesto Clemente-Juan,*^[b] Eugenio Coronado,^[b] Bineta Keita,^[c] Pedro de Oliveira,^[c] Louis Nadjo,*^[c] and Francis Sécheresse^[a]

Abstract: Five Co^{II} silicotungstate complexes are reported. The centrosymmetric heptanuclear compound $K_{20}[\{(B-\beta-SiW_9O_{33}(OH))(\beta-SiW_8O_{29}(OH)_2)Co_3(H_2O)_2\}_2Co(H_2O)_2] \cdot 47 H_2O$ (**1**) consists of two $\{(B-\beta-SiW_9O_{33}(OH))(\beta-SiW_8O_{29}(OH)_2)Co_3(H_2O)_2\}$ units connected by a $\{CoO_4(H_2O)_2\}$ group. In the chiral species $K_7[Co_{1.5}(H_2O)_7][(\gamma-SiW_{10}O_{36})(\beta-SiW_8O_{30}(OH))Co_4(OH)(H_2O)_7] \cdot 36 H_2O$ (**2**), a $\{\gamma-SiW_{10}O_{36}\}$ and a $\{\beta-SiW_8O_{30}(OH)\}$ unit enclose a mononuclear $\{CoO_4(H_2O)_2\}$ group and a $\{Co_3O_7(OH)(H_2O)_5\}$ fragment. The two trinuclear Co^{II} clusters present in **1** enclose a μ_4 -O atom, while in **2** a μ_3 -OH bridging group connects the three paramagnetic centers of the trinuclear unit, inducing significantly larger Co-L-Co ($L = \mu_4$ -O (**1**), μ_3 -OH (**2**)) bridging angles in **2**

($\theta_{av(Co-L-Co)} = 99.1^\circ$) than in **1** ($\theta_{av(Co-L-Co)} = 92.8^\circ$). Weaker ferromagnetic interactions were found in **2** than in **1**, in agreement with larger Co-L-Co angles in **2**. The electrochemistry of **1** was studied in detail. The two chemically reversible redox couples observed in the positive potential domain were attributed to the redox processes of Co^{II} centers, and indicated that two types of Co^{II} centers in the structure were oxidized in separate waves. Redox activity of the seventh Co^{II} center was not detected. Preliminary experiments indicated that **1** catalyzes the reduction of nitrite and NO. Remarkably, a reversi-

ble interaction exists with NO or related species. The hybrid tetranuclear complexes $K_5Na_3[(A-\alpha-SiW_9O_{34})Co_4(OH)_3(CH_3COO)_3] \cdot 18 H_2O$ (**3**) and $K_5Na_3[(A-\alpha-SiW_9O_{34})Co_4(OH)(N_3)_2(CH_3COO)_3] \cdot 18 H_2O$ (**4**) were characterized: in both, a tetrahedral $\{Co_4(L_1)(L_2)_2(CH_3COO)_3\}$ (**3**: $L_1 = L_2 = OH$; **4**: $L_1 = OH$, $L_2 = N_3$) unit capped the $[A-\alpha-SiW_9O_{34}]^{10-}$ trivacant polyanion. The octanuclear complex $K_8Na_8[(A-\alpha-SiW_9O_{34})_2Co_8(OH)_6(H_2O)_2(CO_3)_3] \cdot 52 H_2O$ (**5**), containing two $\{Co_4O_9(OH)_3(H_2O)\}$ units, was also obtained. Compounds **2**, **3**, **4**, and **5** were less stable than **1**, but their partial electrochemical characterization was possible; the electronic effect expected for **3** and **4** was observed.

Keywords: cobalt • electrochemistry • ligand effects • magnetic properties • polyoxometalates

Introduction

The structures of lacunary polyoxometalate ligands^[1] allow the inclusion of well-isolated clusters of transition metal cat-

ions. The number of metallic ions incorporated in the polyoxometalate matrix as well as the size, charge, solubility, and acidity of these molecular metal oxide compounds^[2] can be modulated so that their properties, such as magnetic be-

[a] Dr. L. Lisnard, Dr. P. Mialane, Dr. A. Dolbecq, Dr. J. Marrot, Prof. F. Sécheresse
Institut Lavoisier de Versailles, UMR CNRS 8180
Université de Versailles, 78035 Versailles Cedex (France)
Fax: (+33) 1-3925-4381
E-mail: mialane@chimie.uvsq.fr

[b] Dr. J. M. Clemente-Juan, Prof. E. Coronado
Instituto de Ciencia Molecular, Universidad de Valencia
Poligono La Coma s/n, 46980 Paterna (Spain)
Fax: (+34) 963-544-418
E-mail: juan.m.clemente@uv.es

[c] Dr. B. Keita, Dr. P. de Oliveira, Prof. L. Nadjo
Laboratoire de Chimie Physique, UMR CNRS 8000
Equipe d'Electrochimie et Photoelectrochimie
Université Paris 11, Bâtiment 350, 91405 Orsay Cedex (France)
Fax: (+33) 1-6915-4328
E-mail: nadjo@lcp.u-psud.fr

Supporting information for this article is available on the WWW under <http://www.chemeurj.org/> or from the author. It contains the UV/Vis spectrum of complex **1** and of its oxidized products, and details of gel filtration chromatography experiments performed on **1** and the electrochemical studies of complexes **2**, **3**, **4** and **5**.

havior^[3] or catalytic activity, can be fine-tuned.^[4] Monomeric polyanionic species inserting from one to nine paramagnetic cations have been reported for magnetic polyoxometalates. It is also possible to increase the number of vacancies in the polyoxometalate ligand by assembling diamagnetic polyoxometalate subunits into larger anionic species, and thence to obtain magnetic systems of higher nuclearities.^[5] For example, Kortz et al. have shown recently that the pre-formed tetrameric $[H_7P_8W_{48}O_{184}]^{33-}$ ligand can accommodate 20 Cu^{II} centers connected by hydroxo groups.^[6] On the other hand, the in-situ reaction of multilacunary monomeric polyanions with paramagnetic cations can lead to oligomeric high-nuclearity species. This is generally achieved by acid–base condensation,^[7] but supramolecular assemblies around small anions such as halides can also be effective.^[8] Recently, insertion into paramagnetic polyoxometalate matrices of exogenous ligands and especially that of the azido anion^[9] has shown that such polydentate ligands can also allow the assembly of magnetic polyoxometalate subunits,^[10] but in addition could impose ferromagnetic interactions within the cluster.^[11,12]

Co^{II} polyoxometalate compounds containing from two to nine interacting paramagnetic centers have been reported. The monomeric Keggin complex $[Co(H_2O)(CoW_{11}O_{39})]^{8-}$, consisting of two μ -O-bridged Co^{II} centers in a tetrahedral and an octahedral environment (Figure 1a) was reported in 1956.^[13] More recently, synthesis of dimeric sandwich-type polyoxometalates has made it possible to isolate di-, tri-, tetra-, and pentanuclear Co^{II} compounds. The tetranuclear species are all composed of a $\{Co_4O_{16}\}$ rhomb-like cluster (Figure 1b) encapsulated between two trilacunary Keggin-type $[B-XW_9O_{33}]^{n-}$ ($X = P^V, As^V, n = 7; X = Zn^{II}, n = 10$) or Dawson-type $[X_2W_{15}O_{56}]^{12-}$ ($X = P^V, As^V$) moieties, with all

the cobalt centers in an octahedral environment.^[14] (The A and B nomenclature in this manuscript refer to the different vacancy types found in the Keggin structures.) Related trinuclear compounds are obtained by the formal replacement of a Co^{II} center belonging to the $\{Co_4O_{16}\}$ tetranuclear unit by a tungsten or a sodium cation (Figure 1c).^[15] Analogously, the replacement of two cobalt centers of the $\{Co_4O_{16}\}$ core by two sodium ions leads to a dinuclear Co^{II} sandwich polyoxometalate (Figure 1d).^[15c] The pentanuclear species $[Co_3W(H_2O)_2(CoW_9O_{34})_2]^{12-}$, in which two tetrahedral Co^{II} centers are connected to three octahedral Co^{II} ions by two μ_4 -O atoms (Figure 1e), is also derived from these sandwich-type structures.^[15a,16] Three trimeric Co^{II} phosphotungstate compounds based on the $\{Co_3(B-PW_9O_{34})\}$ building unit in which a triangular $\{Co_3O_{13}\}$ group (Figure 1f) caps the trivalent Keggin anion have also been characterized. The hexa-^[17] and heptanuclear^[18] (Figure 1g) complexes are constructed of two subunits connected by a $[PW_6O_{26}]^{11-}$ fragment and a $[CoW_7O_{26}(OH)_2]^{10-}$ group, respectively, while in the nonanuclear compound the three subunits are linked by two $[HPO_4]^{2-}$ groups (Figure 1h).^[19] In contrast with the hepta- and nonanuclear compounds, in the hexanuclear complex the two $\{Co_3O_{13}\}$ units are pseudo-isolated magnetically.

The chemistry of Co^{II} polyoxometalates with di- or pentavalent heteroatoms has been widely explored; there is a huge diversity of compounds. Surprisingly, it was only in 2005 that the first Co^{II} silicotungstate complexes with magnetically coupled paramagnetic ions were reported. The trinuclear complex^[20] $[Co_3(B-\beta-SiW_9O_{33}(OH))(B-\beta-SiW_8O_{29}(OH)_2)]^{11-}$ contains a $\{Co_3(B-SiW_9O_{34})\}$ unit which can be compared with the $\{Co_3(B-PW_9O_{34})\}$ unit previously mentioned, while the nonanuclear compound^[21] $[Co_9Cl_2(OH)_3(H_2O)_9(\beta-SiW_8O_{31})_3]^{17-}$ is related to the nonanuclear phosphotungstate complex described above, with two chloride anions instead of two protonated phosphato groups connecting the trinuclear units. Pursuing our efforts toward the functionalization of magnetic polyoxometalate compounds by exogenous ligands, we report here the characterization of five new Co^{II} silicotungstate complexes synthesized in the presence of carboxylato, cyanato, azido, and/or carbonato ligands. Both the unfunctionalized species $K_{20}[\{(B-\beta-SiW_9O_{33}(OH))(\beta-SiW_8O_{29}(OH)_2)Co_3(H_2O)_2\}Co(H_2O)_2] \cdot 47H_2O$ (**1**), obtained in the presence of acetato ligands, and $K_7[Co_{1.5}(H_2O)_7][(\gamma-SiW_{10}O_{36})(\beta-SiW_8O_{30}(OH))Co_4(OH)(H_2O)_7] \cdot 36H_2O$ (**2**), obtained in the presence of acetato and cyanato ligands, enclose the triangular $\{Co_3O_{13}\}$ unit represented in Figure 1f, but while in **1** the three Co^{II} centers are connected by a central μ_4 -O ligand arising from a $\{SiO_4\}$ group, the paramagnetic ions are bridged by a μ_3 -OH group in **2**. Whereas these two complexes are related to Co^{II} polyoxoanions including the $\{Co_3O_{13}\}$ fragment,^[17–19] the successful grafting of acetato, azido, or carbonato ligands onto the paramagnetic centers embedded in the polyanionic matrix has afforded complexes inserting paramagnetic clusters unprecedented in the chemistry of Co^{II} polyoxometalates. In the hybrid complex $K_3Na_3[(A-\alpha-SiW_9O_{34})Co_4(OH)_3(CH_3COO)_3] \cdot 18H_2O$ (**3**), a tetrahedral $\{Co_4(OH)_3-$

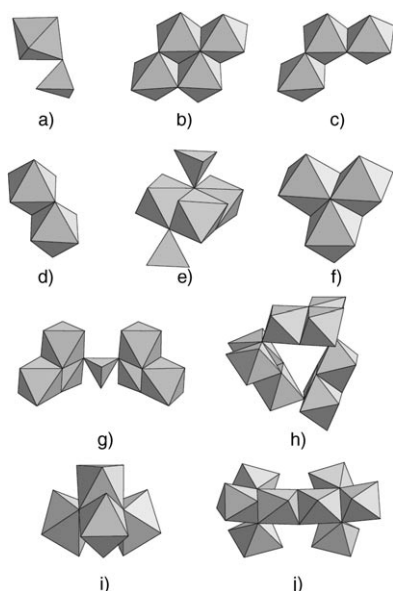


Figure 1. Polyhedral representation of the geometries of (a–h) the polyoxometalate-encapsulated Co^{II} clusters previously reported and (i, j) the new clusters reported herein.

(CH₃COO)₃ unit (Figure 1i) caps the [A- α -SiW₉O₃₄]¹⁰⁻ trivacant polyanion. Two bridging hydroxo ligands can be substituted by two azido anions, leading to K₅Na₃[(A- α -SiW₉O₃₄)Co₄(OH)(N₃)₂(CH₃COO)₃] \cdot 18H₂O (**4**). This complex represents, to the best of our knowledge, the first example of a polyoxometalate compound in which the magnetic centers are connected by two kinds of exogenous polyatomic ligands. In the presence of carbonate, K₈Na₈[(A- α -SiW₉O₃₄)₂Co₈(OH)₆(H₂O)₂(CO₃)₃] \cdot 52H₂O (**5**) has been obtained, corresponding to the first polyoxometalate complex containing a double-tetrahedral Co^{II} unit (Figure 1j). The magnetic properties of complexes **1** and **2** have been investigated, making it possible to determine the exchange coupling constants characterizing these compounds. The stability in solution of all these complexes has been examined by UV/Vis spectroscopy. The stability of **1** in the pH 0–7 domain has allowed its electrochemistry to be studied in detail; preliminary experiments have indicated that this compound catalyzes the reduction of nitrite and NO. Remarkably, the existence of a reversible interaction with NO or related species was observed.

Results and Discussion

Synthesis and IR spectroscopy: The complexes **1** and **2** were both synthesized in water (pH 5) at room temperature by mixing K₈[γ -SiW₁₀O₃₆] \cdot 12H₂O with cobalt acetate (2 equiv). In the case of **2**, potassium cyanate was added to the reacting medium. The decomposition of the precursor into the [B- β -SiW₉O₃₄] and [β -SiW₈O₃₁] units has been observed and discussed previously.^[10,20,21] The [(B- β -SiW₉O₃₃(OH))(β -SiW₈O₂₉(OH)₂)Co₃(H₂O)] unit can be obtained under various reaction conditions (medium, temperature, concentration),^[20] highlighting the stability of this sandwich polyoxometalate entity. While the presence of KNCO has a strong influence on the formation of the resulting compound, the insertion of this ligand into the polyoxometalate matrix has not been achieved. The complex **3** was obtained starting from the Na₁₀[(A- α -SiW₉O₃₄)₂] \cdot 19H₂O precursor in the presence of a stoichiometric amount of Co^{II} in an aqueous solution of potassium acetate (1 M, pH 8) with gentle heating. After removal of an abundant precipitate (**3a**), **3** was obtained as a pure crystalline phase in poor yield from the filtrate. The elemental analysis of the powder^[22] suggested that **3a** is the sandwich-type compound K₁₄[(A- α -SiW₉O₃₄)₂Co₃(H₂O)_{*n*}] \cdot (47-*n*)H₂O, which can be compared with the K₉[(A- α -PW₉O₃₄)₂(Fe(H₂O)₂)₃] \cdot 20H₂O complex reported by Hill et al.^[23] FTIR analysis confirmed the absence of acetato ligands in **3a**, while four bands characteristic of COO vibrations^[24] were found in the 1650–1400 cm⁻¹ range for complex **3** ($\nu_{\text{asym}}=1606$ and 1556 cm⁻¹; $\nu_{\text{sym}}=1443$ and 1421 cm⁻¹). This indicates the presence of two types of non-equivalent acetato ligands. The ν_{asym} and ν_{sym} modes can be correlated by considering the relative intensities of the bands. The calculated Δ values, defined as $\nu_{\text{asym}}-\nu_{\text{sym}}$,^[25] are $\Delta_1=163$ cm⁻¹^[26] and $\Delta_2=135$ cm⁻¹; they suggest a bidentate

bridging mode coordination for both ligands, even if the Δ_1 value is close to that found for the ionic sodium acetato compound ($\Delta=164$ cm⁻¹). The complex **4** was synthesized in good yield under conditions analogous to those used for **3**, except that a threefold excess of sodium azide was added to the reaction medium. Even with a larger excess of the N₃⁻ ion, it was not possible to substitute the three μ_3 -hydroxo ligands present in **3** by three azido ones. The number of grafted azido ligands has been determined by considering both the XRD data and the elemental analysis. FTIR spectroscopy confirmed the presence of equivalent asymmetric azido ligands: a strong ν_{asym} band was observed at 2098 cm⁻¹ and a weak ν_{sym} band appeared at 1283 cm⁻¹.^[24,27] As for **3**, four bands suggesting the presence of non-equivalent bidentate bridging acetato ligands were found in the FTIR spectrum of **4** ($\nu_{\text{asym}}=1594$ and 1555 cm⁻¹, $\nu_{\text{sym}}=1437$ and 1417 cm⁻¹; $\Delta_1=157$ cm⁻¹ and $\Delta_2=138$ cm⁻¹).^[26] The complex K₈Na₈[(A- α -SiW₉O₃₄)₂Co₈(OH)₆(H₂O)₂(CO₃)₃] \cdot 52H₂O (**5**) was synthesized in similar conditions to those used for **4**, but with sodium azide replaced by an excess of potassium carbonate. Its FTIR spectrum showed two intense bands at 1482 and 1379 cm⁻¹, which were ascribed to carbonate-based asymmetric stretching modes.^[28]

Solid-state structures

*K*₂₀[(B- β -SiW₉O₃₃(OH))(β -SiW₈O₂₉(OH)₂)Co₃(H₂O)]₂Co(H₂O)₂ \cdot 47H₂O (**1**): Compound **1** (Figure 2) is composed of two equivalent [(B- β -SiW₉O₃₃(OH))(β -SiW₈O₂₉(OH)₂)Co₃(H₂O)] units which have been described already for the related compound [(B- β -SiW₉O₃₃(OH))(β -SiW₈O₂₉(OH)₂)Co₃(H₂O)]₂²²⁻ (**1a**).^[20] In each subunit, a nearly equilateral triangular {Co₃} cluster is encapsulated between a [B- β -SiW₉O₃₃(OH)]⁹⁻ unit and a [β -SiW₈O₂₉(OH)₂]⁸⁻ fragment. Two {W₃O₁₃} groups of the [(B- β -SiW₉O₃₃(OH))] fragments constituting **1** are disordered over two positions related by a

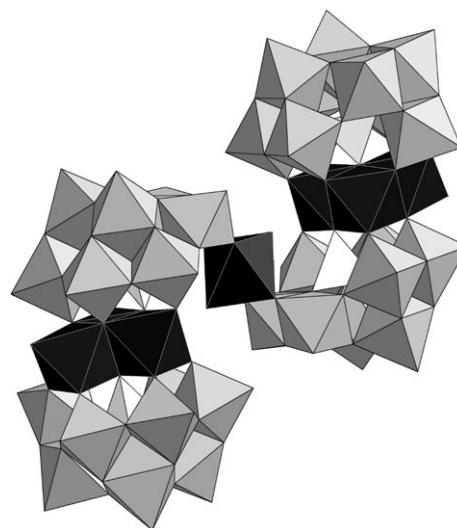


Figure 2. Polyhedral representation of the [(B- β -SiW₉O₃₃(OH))(β -SiW₈O₂₉(OH)₂)Co₃(H₂O)]₂Co(H₂O)₂]²⁰⁻ polyanion in **1**. Gray octahedra, {WO₆}; black octahedra, {CoO₆}; white tetrahedra, {SiO₄}.

60° rotation. For **1** and **1a**, the two $\{(\beta\text{-SiW}_9\text{O}_{33}(\text{OH}))(\beta\text{-SiW}_8\text{O}_{29}(\text{OH})_2)\text{Co}_3(\text{H}_2\text{O})\}$ groups are held by Co-O-W bonds. Nevertheless, while in the chiral compound **1a** the connection between the two subunits occurs through the two trinuclear Co^{II} clusters, in the centrosymmetric compound **1** the connection occurs through a $\{\text{CoO}_4(\text{H}_2\text{O})_2\}$ group, which lies on an inversion center. As a result, whereas in **1a** the two equivalent sandwich fragments are almost orthogonal to each other, a parallel arrangement of the subunits is found in **1**. The number of potassium counterions in **1**, determined by elemental analysis, indicates that this complex is hexaprotonated and, in agreement with calculations performed on **1a**,^[20] bond valence sum calculations^[29] (BVSC) indicate that the protons are located on μ_2 -bridging oxygen atoms.

$K_7[\text{Co}_{1.5}(\text{H}_2\text{O})_7][(\gamma\text{-SiW}_{10}\text{O}_{36})(\beta\text{-SiW}_8\text{O}_{30}(\text{OH}))\text{Co}_4(\text{OH})(\text{H}_2\text{O})_7]\cdot 36\text{H}_2\text{O}$ (**2**): Complex **2** is built from a $[\gamma\text{-SiW}_{10}\text{O}_{36}]^{8-}$ and a $[\beta\text{-SiW}_8\text{O}_{30}(\text{OH})]^{9-}$ Keggin unit connected by a mononuclear $\{\text{CoO}_4(\text{H}_2\text{O})_2\}$ group and a $\{\text{Co}_3\text{O}_7(\text{OH})(\text{H}_2\text{O})_5\}$ fragment (Figure 3). The $\{\text{CoO}_4(\text{H}_2\text{O})_2\}$ unit is coor-

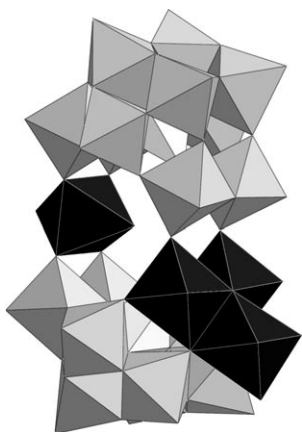


Figure 3. Polyhedral representation of the $[(\gamma\text{-SiW}_{10}\text{O}_{36})(\beta\text{-SiW}_8\text{O}_{30}(\text{OH}))\text{Co}_4(\text{OH})(\text{H}_2\text{O})_7]^{10-}$ polyanion in **2**. Gray octahedra, $\{\text{WO}_6\}$; black octahedra, $\{\text{CoO}_6\}$; white tetrahedra, $\{\text{SiO}_4\}$.

ordinated to two oxygen atoms of the $[\gamma\text{-SiW}_{10}\text{O}_{36}]^{8-}$ polyoxometalate and two oxygen atoms of the $[\beta\text{-SiW}_8\text{O}_{30}(\text{OH})]^{9-}$ polyanion, while the $\{\text{Co}_3\text{O}_7(\text{OH})(\text{H}_2\text{O})_5\}$ fragment is dicoordinated to the divacant Keggin unit and pentacoordinated to the tetravacant polyoxotungstate ligand. Five water ligands complete the coordination sphere of these octahedral paramagnetic ions. A central μ_3 -hydroxo ligand $[\text{BVSC}(\mu_3\text{-O}(\text{H})) = 1.09]^{[29]}$ connects the cobalt centers. An additional $\{\text{CoO}_3(\text{H}_2\text{O})_3\}$ group (Figure S1) with an occupation factor of 0.5 is coordinated by three μ -oxo atoms to the tetravacant Keggin unit, capping the $[\beta\text{-SiW}_8\text{O}_{30}(\text{OH})]^{9-}$ fragment. Elemental analysis data and electroneutrality considerations led us to propose that this $\{\text{CoO}_3(\text{H}_2\text{O})_3\}$ group is disordered together with two protons. Then, **2** can be described as the superposition of the $[(\gamma\text{-SiW}_{10}\text{O}_{36})(\beta\text{-SiW}_8\text{O}_{31}\text{Co}(\text{H}_2\text{O})_3)\text{Co}_4(\text{OH})(\text{H}_2\text{O})_7]^{9-}$ and $[(\gamma\text{-SiW}_{10}\text{O}_{36})(\beta\text{-SiW}_8\text{O}_{29}(\text{OH})_2)\text{Co}_4-$

$(\text{OH})(\text{H}_2\text{O})_7]^{9-}$ units. Due to the disorder, it has not been possible to support the presence of the protons by bond valence sum calculations, but the charge stated for the $\{\beta\text{-SiW}_8\text{O}_{31}\}$ fragment in **2** does agree with that found for the same subunit in the complexes **1** and **1a**. The presence of a supplementary Co^{II} ion capping this Keggin unit indicates, as postulated by Kortz et al.,^[20] that it is possible to connect additional metallic atoms to the surface of the $\{\beta\text{-SiW}_8\text{O}_{31}\}$ group after filling its vacancies, highlighting the basicity of this fragment. Interestingly, it is the first time that such a triangular $\{\text{Co}_3\}$ fragment connected to a polyoxometalate ligand has been found to enclose a central μ_3 -OH ligand; all the analogous compounds previously characterized possessed a central μ_4 -O belonging to an $\{\text{XO}_4\}$ hetero group ($\text{X} = \text{P}^{\text{V}}, \text{Si}^{\text{IV}}$). This induces a noticeable increase in the Co-L-Co angles ($\text{L} = \mu_4\text{-O}$ in **1** and **1a**, and $\mu_3\text{-OH}$ in **2**; $\theta_{\text{av}(\text{Co-L-Co})} = 92.8^\circ$ in **1**, 92.9° in **1a**, and 99.1° in **2**). On the other hand, the protonation of the central oxygen atom does not significantly influence the Co-O-Co angles involving the peripheral oxo ligands ($\theta_{\text{av}(\text{Co-O-Co})} = 93.9^\circ$ in **1**, 93.4° in **1a**, and 94.7° in **2**). Very few sandwich-type polyoxometalate compounds containing two different Keggin units have been characterized. Apart from **1** and **1a**, $[\text{Zr}(\text{PMO}_{12}\text{O}_{40})(\text{PMO}_{11}\text{O}_{39})]^{6-}$ ^[30] and $[\text{Ni}_7(\text{OH})_4(\text{H}_2\text{O})(\text{CO}_3)_2(\text{HCO}_3)(\text{A-}\alpha\text{-SiW}_9\text{O}_{34})(\beta\text{-SiW}_{10}\text{O}_{37})]^{10-}$ ^[31] represent the first sandwich-type polyanions made from a divacant and a tetravacant polyoxoanion.

$K_5\text{Na}_3[(\text{A-}\alpha\text{-SiW}_9\text{O}_{34})\text{Co}_4(\text{OH})_3(\text{CH}_3\text{COO})_3]\cdot 18\text{H}_2\text{O}$ (**3**) and $K_5\text{Na}_3[(\text{A-}\alpha\text{-SiW}_9\text{O}_{34})\text{Co}_4(\text{OH})(\text{N}_3)_2(\text{CH}_3\text{COO})_3]\cdot 18\text{H}_2\text{O}$ (**4**):

Compound **3** can be described as a $[\text{A-}\alpha\text{-SiW}_9\text{O}_{34}]^{10-}$ trivacant polyanion accommodating a $\{\text{Co}_3(\mu_3\text{-OH})_3\}$ fragment, each cobalt center being tricoordinated to the polyoxotungstate. A fourth Co^{II} ion connected to these paramagnetic centers through three μ_2 -acetato ligands caps the trinuclear fragment (Figure 4). All the Co^{II} centers are thus in an octahedral environment. While the overall symmetry of **3** is close to C_3 , the crystallographic symmetry of the $[(\text{A-}\alpha\text{-SiW}_9\text{O}_{34})\text{Co}_4(\text{OH})_3(\text{CH}_3\text{COO})_3]^{8-}$ unit is C_s , with a mirror plane containing the Co2, Co3, and silicon atoms intersect-

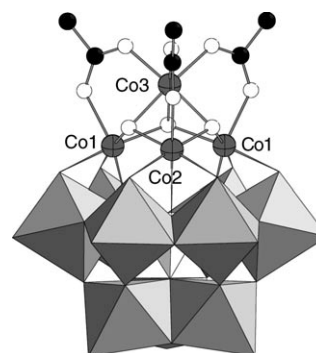


Figure 4. Polyhedral and ball-and-stick representation of the $[(\text{A-}\alpha\text{-SiW}_9\text{O}_{34})\text{Co}_4(\text{OH})_3(\text{CH}_3\text{COO})_3]^{8-}$ polyanion in **3**. Gray octahedra, $\{\text{WO}_6\}$; white tetrahedra, $\{\text{SiO}_4\}$; gray cross-hatched spheres, Co; black spheres, C; white spheres, O.

ing the polyanion. It follows that only two of the three acetato ligands are crystallographically equivalent, in agreement with the IR data. For the Co1 and Co2 centers, the equatorial plane is defined by two O(W) atoms of the $[\text{A-}\alpha\text{-SiW}_9\text{O}_{34}]^{10-}$ unit and two hydroxo groups ($d_{\text{Co-OH}}=2.022(5)\text{--}2.046(9)\text{ \AA}$; $\text{Co-O(H)-Co}=130.3(5)^\circ$ and $132.4(7)^\circ$), the apical positions being occupied by an O(Si) atom ($d_{\text{Co-O}_{\text{Si}}}=2.280(10)$ and $2.328(14)\text{ \AA}$) and an oxygen atom of an acetato ligand ($d_{\text{Co-OOCH}_3}=2.107(16)$ and $2.136(12)\text{ \AA}$). Considering the Co3 center, the two Co3-OH bonds involving the two hydroxo groups connecting the three crystallographically independent cobalt centers are long ($d_{\text{Co-OH}}=2.116(9)\text{ \AA}$, $\text{Co-O(H)-Co}=91.4(4)^\circ$ and $91.7(4)^\circ$), the four other bonds being in the range $2.067(11)\text{--}2.080(13)\text{ \AA}$ ($\text{Co-O(H)-Co}=93.4(4)^\circ$). The structure of **4** is derived from that of **3**, with two $\mu_{1,1,1}$ -azido ligands replacing two μ_3 -hydroxo bridges (Figure 5). In **4**, a C_3 axis contains the silicon and the Co2

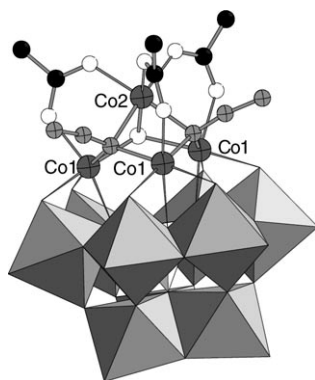


Figure 5. Polyhedral and ball-and-stick representation of the $[(\text{A-}\alpha\text{-SiW}_9\text{O}_{34})\text{Co}_4(\text{OH})(\text{N}_3)_2(\text{CH}_3\text{COO})_3]^{8-}$ polyanion in **4**. Gray octahedra, $\{\text{WO}_6\}$; white tetrahedra, $\{\text{SiO}_4\}$; gray cross-hatched spheres, Co; black spheres, O; light gray cross-hatched spheres, N; white spheres, O.

centers, inducing a crystallographic disorder between the μ_3 -ligands L' ($L'=\text{N}_3^-, \text{OH}^-$) bridging the three Co^{II} ions embedded in the polyoxometalate matrix ($d_{\text{Co1-L}'}=2.072(5)\text{ \AA}$ and $d_{\text{Co2-L}'}=2.114(4)\text{ \AA}$; $\text{Co1-L}'\text{-Co1}=129.4(2)^\circ$ and $\text{Co1-L}'\text{-Co2}=91.60(16)^\circ$). Complex **4** can also be regarded as a dimeric compound, a sodium ion hexacoordinated to six oxygen atoms of six acetato ligands ensuring the connection between two $[(\text{A-}\alpha\text{-SiW}_9\text{O}_{34})\text{Co}_4(\text{OH})(\text{N}_3)_2(\text{CH}_3\text{COO})_3]^{8-}$ subunits (Figure S2). Few polyoxometalates containing bridging carboxylato ligands have been reported.^[7,32] Moreover, **3** and **4** represent rare cases of tetranuclear complexes capping a Keggin-type polyanion,^[33] but the $\{\text{Co}_4\text{O}_9\text{L}_3\text{-}(\text{CH}_3\text{COO})_3\}$ tetrahedral cluster can be compared with the $[\text{Ni}_4\text{O}_9(\text{OH})_3(\text{CO}_3)_3]$ tetranuclear unit found in the complex $[\text{Ni}_7(\text{OH})_4(\text{H}_2\text{O})(\text{CO}_3)_2(\text{HCO}_3)(\text{A-}\alpha\text{-SiW}_9\text{O}_{34})(\beta\text{-SiW}_{10}\text{O}_{37})]^{10-}$.^[31]

$K_8\text{Na}_8[(\text{A-}\alpha\text{-SiW}_9\text{O}_{34})_2\text{Co}_8(\text{OH})_6(\text{H}_2\text{O})_2(\text{CO}_3)_3]\cdot 52\text{H}_2\text{O}$ (**5**): The octanuclear compound **5** can be described as two $\{(\text{A-}\alpha\text{-SiW}_9\text{O}_{34})\text{Co}_4(\text{OH})_3(\text{H}_2\text{O})\}$ subunits connected through

three carbonato groups (Figure 6). Two crystallographically independent $[(\text{A-}\alpha\text{-SiW}_9\text{O}_{34})_2\text{Co}_8(\text{OH})_6(\text{H}_2\text{O})_2(\text{CO}_3)_3]^{16-}$ entities are found in the unit cell. A pseudo-mirror plane containing the carbon atoms of the carbonato ligands relates

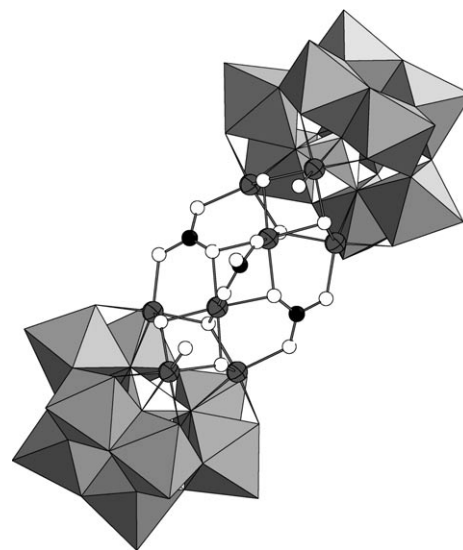


Figure 6. Polyhedral and ball-and-stick representation of the $[(\text{A-}\alpha\text{-SiW}_9\text{O}_{34})_2\text{Co}_8(\text{OH})_6(\text{H}_2\text{O})_2(\text{CO}_3)_3]^{16-}$ polyanion in **5**. Gray octahedra, $\{\text{WO}_6\}$; white tetrahedra, $\{\text{SiO}_4\}$; gray cross-hatched spheres, Co; black spheres, O; white spheres, O.

the two $\{(\text{A-}\alpha\text{-SiW}_9\text{O}_{34})\text{Co}_4(\text{OH})_3(\text{H}_2\text{O})\}$ groups. The tetranuclear subunit can be compared to the $[(\text{A-}\alpha\text{-SiW}_9\text{O}_{34})\text{Co}_4(\text{OH})_3(\text{CH}_3\text{COO})_3]^{8-}$ unit found in **3** and **4**. As in these compounds, a $\{\text{Co}_3(\mu_3\text{-OH})_3\}$ fragment completes the trivacant $[\text{A-}\alpha\text{-SiW}_9\text{O}_{34}]^{10-}$ ligand ($d_{\text{Co-OH}}=2.035(8)\text{--}2.073(7)\text{ \AA}$; $\text{Co-O(H)-Co}=126.8(4)\text{--}132.5(4)^\circ$), the three μ_3 -OH ligands also being connected to a Co^{II} ion capping the trinuclear group ($d_{\text{Co-OH}}=2.086(7)\text{--}2.132(7)\text{ \AA}$; $\text{Co-O(H)-Co}=90.6(3)\text{--}97.9(3)^\circ$). Two $\mu_4\text{-}\eta^1\text{:}\eta^1\text{:}\eta^2$ CO_3^{2-} ligands ensure the connection of a Co^{II} center of the $\{\text{Co}_3(\mu_3\text{-OH})_3\}$ unit to the apical Co^{II} ion, but additionally to the corresponding Co^{II} centers of the adjacent subunit ($d_{\text{Co-OCO}_2}=2.069(8)\text{--}2.116(8)\text{ \AA}$). The third carbonato group acts as a $\mu_2\text{-}\eta^1\text{:}\eta^1$ ligand, connecting the two apical Co^{II} ions of the two tetrahedral $\{\text{Co}_4\}$ units ($d_{\text{Co-OCO}_2}=2.032(8)\text{--}2.059(9)\text{ \AA}$). Such an arrangement is close to that found in the carbonato heptanuclear Ni^{II} complex $[\text{Ni}_7(\text{OH})_4(\text{H}_2\text{O})(\text{CO}_3)_2(\text{HCO}_3)(\text{A-}\alpha\text{-SiW}_9\text{O}_{34})(\beta\text{-SiW}_{10}\text{O}_{37})]^{10-}$ reported recently.^[31] It is likely that in **5** the $\mu_2\text{-}\eta^1\text{:}\eta^1$ carbonato ligand is deprotonated, the C–O bond involving the terminal oxygen being significantly shorter ($d_{\text{C-O}}=1.272(16)$ and $1.277(14)\text{ \AA}$) than those found for similar protonated groups ($1.35 < d_{\text{C-O}} < 1.50\text{ \AA}$).^[34] A water molecule completes the coordination sphere of the two Co^{II} ions not bonded to a carbonato ligand.

Magnetic properties: Both $\chi_{\text{M}}T$ versus T curves of **1** and **2** (Figures 7 and 8, respectively) exhibit a continuous decrease from room temperature ($\chi_{\text{M}}T=43.1\text{ emu K mol}^{-1}$ for **1** and $30.7\text{ emu K mol}^{-1}$ for **2**) to a minimum at 42 K. Below this

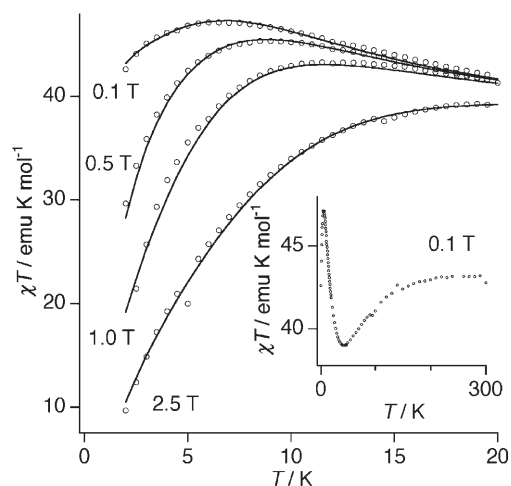


Figure 7. Thermal behavior of $\chi_M T$ for **1** at different fields: 0.1, 0.5, 1, and 2.5 T in the range 2–20 K. Inset: experimental $\chi_M T$ of the same sample at 0.1 T in the range 2–300 K.

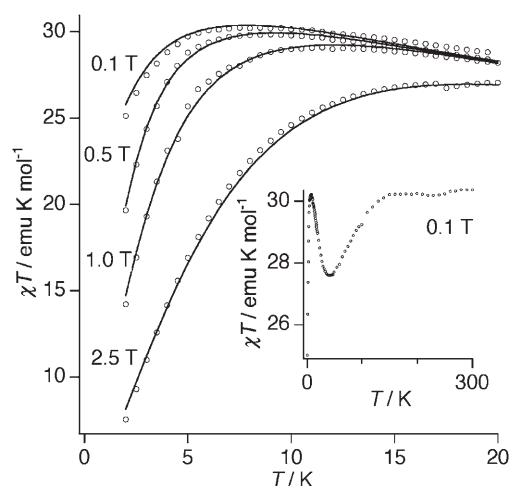


Figure 8. Thermal behavior of $\chi_M T$ for **2** at different fields (0.1, 0.5, 1, and 2.5 T) in the range 2–20 K. Inset: experimental $\chi_M T$ of the same sample at 0.1 T in the range 2–300 K.

temperature, a sharp peak is observed with a maximum at 6.5 K for **1** ($\chi_M T = 47.2 \text{ emu K mol}^{-1}$) and at 7.5 K for **2** ($\chi_M T = 30.3 \text{ emu K mol}^{-1}$). These maxima clearly depend on the magnetic field (Figures 7 and 8). When the magnetic field increases, the maximum decreases in value and becomes broader. The decrease from room temperature can be attributed to the spin–orbit coupling of Co^{II} . The Co^{II} atom in an octahedral coordination has a high-spin ground state 4T_1 with first-order spin–orbit coupling. This ground state is split into six anisotropic Kramers doublets. At low temperature when the $\chi_M T$ versus T curves present a peak only the lowest Kramers doublet is populated. This indicates that the ferromagnetic ground state for the clusters is due to the anisotropic exchange between the lowest Kramers doublets with effective spins 1/2.

Taking into account all the aspects mentioned above, the effective exchange Hamiltonian for compounds **1** and **2** can be written as Equation (1), in which J is the only exchange pathway involved if we suppose that the three Co^{II} in the trinuclear units are equivalent.

$$\hat{H} = -2 \sum_{\alpha=x,y,z} J_{\alpha} (\hat{S}_1^{\alpha} \hat{S}_2^{\alpha} + \hat{S}_1^{\alpha} \hat{S}_3^{\alpha} + \hat{S}_2^{\alpha} \hat{S}_3^{\alpha}) \quad (1)$$

This exchange Hamiltonian is valid for both compounds and we need only to add the contributions of the isolated Co^{II} units in the appropriate ratio. A simultaneous fit of the four magnetic susceptibilities at different fields was performed by numerical diagonalization of the full eigenmatrix^[35] and gives the following sets of parameters for each compound: $J_z = 11.4 \text{ cm}^{-1}$, $J_x = 9.1 \text{ cm}^{-1}$, $J_y = 7.3 \text{ cm}^{-1}$, $g_z = 5.77$ and $g_{xy} = 4.85$ ($R = 3.4 \times 10^{-5}$)^[36] for **1** and $J_z = 9.8 \text{ cm}^{-1}$, $J_x = 5.2 \text{ cm}^{-1}$, $J_y = 3.9 \text{ cm}^{-1}$, $g_z = 7.64$ and $g_{xy} = 4.69$ ($R = 3.8 \times 10^{-4}$)^[36] for **2**.

The ferromagnetic sign of the exchange parameter can be explained by the orthogonality of the magnetic orbitals in the edge-sharing CoO_6 octahedra (Co–O–Co angles close to 90°). The magnitude of the exchange parameters falls in the range of values found in other related systems with polyoxotungstates encapsulating Co^{II} ions.^[14e, 15b, d, 20] Nevertheless, the intensity of the ferromagnetic coupling is higher for **1** than for **2**. This can be justified easily by considering that the Co–(μ_3 -L)–Co angles (L = OH, O) are significantly larger in **2** than in **1** ($\theta_{\text{av}(\text{Co}-(\mu_3\text{-L})\text{-Co})} = 99.1^\circ$ in **2** and 92.8° in **1**).

Electrochemical experiments

Cyclic voltammetry: All the compounds studied in this section have both tungsten and cobalt centers the electrochemical activities of which become apparent in quite distinct potential domains. For clarity, the phenomena observed in the negative and positive potential domains (versus SCE) are described separately. The phenomena observed in one domain had a negligible influence on those in the other domain.

UV/Vis spectrophotometry showed that **1** is stable in media at pH 0–7 over at least 24 h. The possibilities of **1** breaking down into two monomers or of a Co^{II} atom falling out of the main polyoxometalate structure have been ruled out by gel filtration chromatography (see Supporting Information).

To investigate the reduction of W centers, two cyclic voltammograms were obtained at pH 3 and pH 5 for complex **1** (Figure 9a). In both media, these waves were close to the potential limit imposed by the buffer; they were chemically reversible, which is usual for the electrochemical behavior of the majority of polyoxometalates. When the pH was decreased from 5 to 3, the wave shifted toward the positive potentials, an indication that protons were involved in the reduction process. Since no electron-transfer kinetics study of this type of phenomenon was carried out, it was not possible to correlate the cathodic peak potential shift of 75 mV per

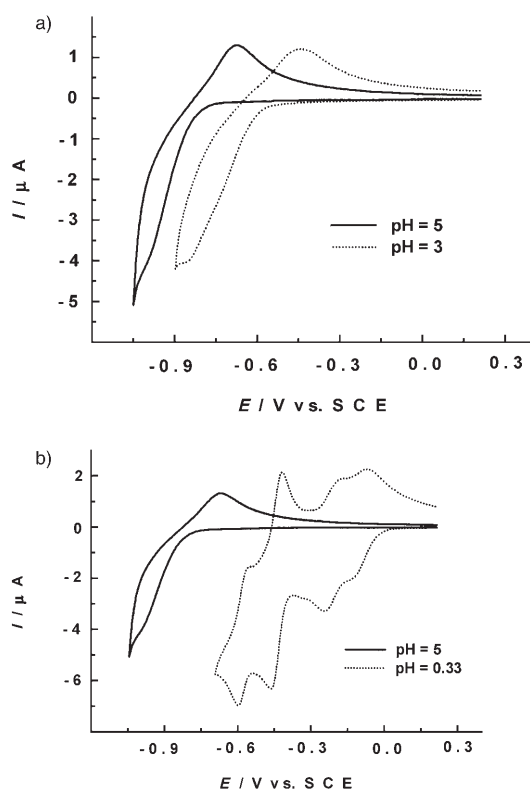


Figure 9. Cyclic voltammograms of 2×10^{-4} M complex **1** obtained in three media at different pH values, addressing just the redox processes of the W centers. The scan rate was 10 mVs^{-1} , and the reference a saturated calomel electrode. a) Comparison of the voltammograms obtained at pH 3 and pH 5; b) comparison of the voltammograms at pH 0.33 and pH 5.

pH unit with the number of protons participating in the reduction. A careful analysis of Figure 9a reveals an incipient cathodic wave splitting for the curve obtained at pH 3.

In Figure 9b, two cyclic voltammograms obtained at pH 0.33 and pH 5 are compared: at pH 0.33 four chemically reversible waves were obtained, the reduction peak potentials of which were -0.142 , -0.250 , -0.476 , and -0.604 V versus SCE. The first two may be considered to have replaced the single wave observed at pH 5. This remarkable phenomenon confirms and amplifies the splitting trend noticed in the voltammogram obtained at pH 3. It is paradoxical that W waves coalesce more frequently than they split when the buffer pH is decreased. This unusual behavior as a function of pH has already been mentioned in the literature.^[21,37] It may be rationalized by the inversion of several pK_a values in the reduced forms of polyoxometalates. Acidity inversion has been demonstrated for various reduced species of 18-molybdo-2-arsenate.^[37b] The same phenomenon has been observed for the crown heteropolyanion $[\text{H}_7\text{P}_8\text{W}_{48}\text{O}_{184}]^{33-}$ ^[37c] and the satellite-shaped compound $[\text{Co}_6(\text{H}_2\text{O})_{30}\{\text{Co}_9\text{Cl}_2(\text{OH})_3(\text{H}_2\text{O})_9(\beta\text{-SiW}_8\text{O}_{31})_3\}]^{5-}$.^[21] The pK_a inversion may well be the general explanation for such a behavior in electrochemistry. The W waves of **1** show strong analogies in both the potential position and the behavior with the complex $[\text{Co}_6(\text{H}_2\text{O})_{30}\{\text{Co}_9\text{Cl}_2(\text{OH})_3(\text{H}_2\text{O})_9(\beta\text{-$

$\text{SiW}_8\text{O}_{31})_3\}]^{5-}$ and also with “banana”-type complexes such as $[\text{Ni}_6\text{As}_3\text{W}_{24}\text{O}_{94}(\text{H}_2\text{O})_2]^{17-}$ and $[\text{Ni}_4\text{Mn}_2\text{P}_3\text{W}_{24}\text{O}_{94}(\text{H}_2\text{O})_2]^{17-}$.^[38] Such analogies are useful in order to estimate the number of electrons involved in each W wave by comparing the peak current intensities recorded under identical experimental conditions. Although potential-controlled coulometry is feasible with the analogues mentioned above, it is impossible to perform it on the single W wave of **1** observed at pH 5: in this case, and even when the potential was set to -0.950 V (that is, roughly 100 mV before the peak maximum), proton reduction catalysis led to consumption of over 41 electrons per molecule. In summary, this proton reduction catalysis carried out by the **1** reduced species prevents determination of the number of electrons involved in the W center wave by coulometry in this medium.

At pH 5, two chemically reversible couples were observed in the positive potential domain versus SCE voltammogram (Figure 10a). The anodic (E_{pa}) and cathodic (E_{pc}) peak potentials for these couples were: $E_{\text{pa}1} = +0.852$ V; $E_{\text{pc}1} = +0.758$ V; $E_{\text{pa}2} = +1.028$ V; $E_{\text{pc}2} = +0.948$ V. These two waves were assigned to processes involving the Co^{II} centers of **1**, as confirmed by potential-controlled coulometry. Indeed, a first oxidation carried out at $+0.860$ V, just beyond the oxidation peak of the first redox couple, took 2.0 ± 0.1 electrons per molecule, and the solution color changed from pale pink to peach. This solution was stable under an argon atmos-

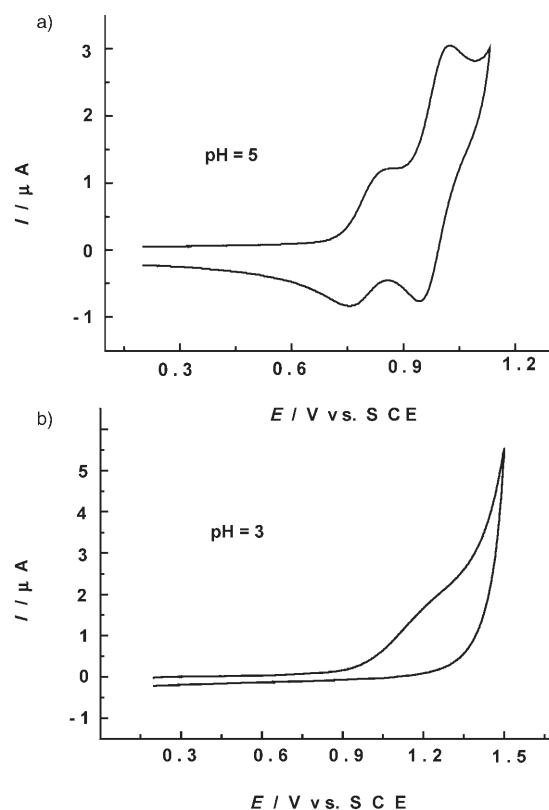


Figure 10. Cyclic voltammograms of 2×10^{-4} M complex **1**, addressing just the redox processes of the Co^{II} centers, obtained in two media with different pH values. The scan rate was 10 mVs^{-1} , and the reference a saturated calomel electrode. a) pH 5; b) pH 3.

where, and when it was submitted to cyclic voltammetry only the features of the second redox couple remained unchanged. When this solution was subjected to a second electrolysis at an imposed potential of +1.050 V, a value slightly more positive than the oxidation peak potential of the second redox couple, the peach color darkened as the reaction proceeded. This oxidation required 4.2 ± 0.1 electrons per molecule, and these results are in agreement with the oxidation current ratio that may be calculated from Figure 10a. When the re-reduction processes were carried out, the final voltammogram retraced the one obtained at the beginning of the experiment, the intensity and the potential position of the waves being identical in both cases. All of these results taken together led to the following conclusions: 1) the redox activity of the seventh Co^{II} has not been detected and 2) the other six Co^{II} centers may be oxidized to Co^{III} , in two distinct groups, in quasi-reversible electron-transfer steps. The separation of the oxidation processes into two different groups must be attributed to the existence of two distinct types of Co^{II} centers in the structure. Hence, the first wave observed when varying the potential toward more positive values was bi-electronic, and may represent the redox behavior of two structurally identical Co^{II} atoms; the second wave, which involved four electrons, must be associated with the other four Co^{II} atoms, which are also structurally identical. To the best of our knowledge, these observations concerning **1** constitute a second example, after that of complex $[\{\text{Co}_3(\text{B}-\beta\text{-SiW}_9\text{O}_{33}(\text{OH}))(\text{B}-\beta\text{-SiW}_8\text{O}_{29}(\text{OH})_2\}_2]^{22-}$,^[20] multi-substituted Co^{II} center polyoxometalates exhibit almost reversible electrochemical behavior. In summary, starting from **1**, which will henceforth be written $(\text{Co}^{\text{II}})_7$ for clarity, the mixed-valence compounds $(\text{Co}^{\text{III}})_2(\text{Co}^{\text{II}})_5$ and $(\text{Co}^{\text{III}})_6(\text{Co}^{\text{II}})$ have been obtained successively. Spectroelectrochemistry experiments confirmed that these three compounds were different. These three species were stable enough in the reaction media to be characterized by their UV/Vis spectra (see Figure S3). Before the electrolysis, the $(\text{Co}^{\text{II}})_7$ spectrum was characterized by a well-defined band at 550 nm, followed by a slight shoulder around 525 nm. The spectrum of $(\text{Co}^{\text{III}})_6(\text{Co}^{\text{II}})$ also exhibited a well-defined band but at 725 nm, and in the intermediate case of the mixed-valence $(\text{Co}^{\text{III}})_2(\text{Co}^{\text{II}})_5$, bands at 725 and 550 nm were observed, with the above-mentioned shoulder at 525 nm. A six-electron complete re-reduction of $(\text{Co}^{\text{III}})_6(\text{Co}^{\text{II}})$ at 0.0 V regenerates a product with the same UV/Vis spectrum as $(\text{Co}^{\text{II}})_7$. Since these compounds are stable, it would be interesting to isolate the $(\text{Co}^{\text{III}})_2(\text{Co}^{\text{II}})_5$ and $(\text{Co}^{\text{III}})_6(\text{Co}^{\text{II}})$ forms in order to study them by X-ray crystallography and to verify that the structure remains that of **1**.

Electrocatalysis: Compound **1** was tested for its electrocatalytic properties regarding the reduction of NO_x . As far as NO_3^- is concerned, no changes, or very small ones, occurred in the voltammograms even at $\gamma = 1000$ (the excess parameter γ is defined as $\gamma = C_{\text{substrate}}^0 / C_{\text{POM}}^0$).

The situation was rather different with NO_2^- : in 0.5 M H_2SO_4 (pH 0.33), this anion was reduced catalytically at the

first wave, with a peak at -0.100 V (at 2 mV s^{-1}) and saturation reached for $\gamma = 20$, for which a current increase of over 30-fold was observed when compared with the situation without NO_2^- . In 0.2 M Na_2SO_4 (pH 3.00 buffer), similar behavior was observed, with a peak potential at -0.640 V (at 2 mV s^{-1}) for $\gamma = 20$, corresponding to a current increase of over 20-fold. This decrease in current intensity as the pH increases is classical for numerous POMs^[37c] and is not shown in detail here. The following sequence is known: $\text{HNO}_2 \rightleftharpoons \text{H}^+ + \text{NO}_2^-$ ($\text{p}K_a = 3.3$ at 18°C) and HNO_2 disproportionates in fairly acidic solution: $3\text{HNO}_2 \rightleftharpoons \text{HNO}_3 + 2\text{NO} + \text{H}_2\text{O}$. The rate of this reaction is known to be low. This designates HNO_2 and NO as the main active species in the pH media.^[37c]

Interestingly, the presence of oxygen in the electrochemical cell led to a decrease in the catalytic current in both buffers, hinting again at the participation of a transitory NO adduct. Experiments carried out with this species (NO -saturated solutions; NO concentration falling between 1 and 2 mM) revealed a pronounced catalytic current which evolved with time (Figure 11). In 0.5 M H_2SO_4 (pH 0.33), the

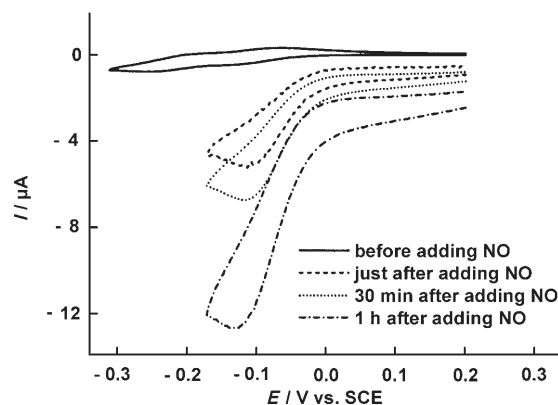


Figure 11. Cyclic voltammograms of 10^{-4} M complex **1**, addressing just the first redox processes of the W centers, without NO and at several time intervals after saturation with NO ($[\text{NO}] = 1\text{--}2$ mM). The scan rate was 2 mV s^{-1} , and the reference a saturated calomel electrode.

reduction peak was at -0.110 V, immediately after the solution had been saturated with NO , and the current increased 10-fold compared with the situation without NO . This new peak was roughly 30 mV more positive than the former first W wave. This hints at the formation of a complex between **1** and NO or a related species. The response evolved with time; the current ratio was over 50:1 after 3 h. The time-dependence profile suggested the existence of an induction period. In addition, the baseline current drifted to increasingly negative values with time, a behavior indicative of changes in the nature of the electrode surface, and therefore of the electric double layer. Such surface phenomena must operate,^[37c] as was seen previously in this work during the electrocatalysis of nitrite reduction, or even with NO alone. They are particularly enhanced in the presence of **1** and NO . These processes were shown to be perfectly reversible, since

the curves obtained at the beginning of the experiment and after the NO had been driven out of the solution by bubbling with argon were virtually the same (Figure S4). Hence, if a complex forms it has to be labile, since the effect of NO is suppressed by bubbling with argon. Similar behavior was observed for saturated polyoxometalates such as $[P_2W_{18}O_{62}]^{6-}$ and $[SiW_{12}O_{40}]^{4-}$, but in these cases the current increase was not so pronounced and there was no noticeable activation of the reduction of NO. Maybe the nature of **1** is more suitable for an interaction with NO with subsequent catalysis of its reduction, but further studies are required before other conclusions can be drawn. The currents measured for NO in the absence of **1** under the same experimental conditions at -0.130 V were negligible.

In 1 M CH_3CO_2Li/CH_3CO_2H (pH 4.00), **1** gave rise to a redox process with a reduction wave at -0.840 V. Under these experimental conditions, NO exhibited a very large reduction wave (with a peak at -0.890 V at 10 mVs $^{-1}$), and the voltammograms were subsequently reversed at -0.600 V. At this potential, the reduction current obtained with both **1** and NO present in the solution was roughly two times that measured with NO alone. Interestingly, the response remained very stable over 3 h, while in the case of NO alone a loss of 25% was observed. NO was removed from the solution upon bubbling with argon, but whereas one hour was sufficient to eliminate it in the absence of **1**, at least two hours were needed when the polyoxometalate was present.

Complex **1** shows the most complete and typical set of properties and behaviors. For all the other POMs containing cobalt described in this paper, UV/Vis spectrophotometry studies revealed a low stability. Nevertheless, partial electrochemical characterization of these compounds was possible. As in the preceding studies, the waves associated with the W and the Co centers have been addressed separately. The most convenient media were chosen for each compound. The corresponding details are described in the Supporting Information.

Conclusion

Five new Co^{II}-silicotungstate complexes have been synthesized starting from the $[A-\alpha-SiW_9O_{34}]^{10-}$ and $[\gamma-SiW_{10}O_{36}]^{8-}$ precursors. In the experimental conditions used here, the divacant polyoxometalate ligand may decompose into the $\{\beta-SiW_8O_{31}\}$ and/or $\{B-\beta-SiW_9O_{34}\}$ units. The two sandwich-type compounds **1** and **2** enclose the trinuclear Co^{II} cluster $\{Co_3O_{13}\}$, with a central μ_4-O atom and a μ_3-OH group, respectively. This difference induces a weakening of the ferromagnetic interactions in **2** compared with **1**. The stability of **1** in solution has allowed its electrochemistry to be studied in detail. Preliminary experiments with NO_x indicate that **1** catalyzes the reductions of nitrite and NO. The remarkable existence of a reversible interaction with NO or related species has been observed. Complex **1** also has potential applications in catalysis and electrocatalysis due to the reversible

behavior of its Co^{II} centers. Starting from the $[A-\alpha-SiW_9O_{34}]^{10-}$ polyoxometalate, two tetranuclear complexes with $\{Co_4(L^1)(L^2)_2(CH_3COO)_3\}$ units ($L^1=L^2=OH$ (**3**); $L^1=OH, L^2=N_3$ (**4**)) capping the trivacant polyanion have been obtained, confirming the higher stability of this polyanion than the $[\gamma-SiW_{10}O_{36}]^{8-}$ precursor. The octanuclear complex **5** with carbonato groups bridging the paramagnetic centers has also been obtained. Such tetrahedral (**3** and **4**) and double-tetrahedral (**5**) paramagnetic clusters have never been observed previously in Co^{II} polyoxometalate chemistry; their presence highlights the fact that the inclusion of exogenous ligands in polyoxometalate matrices allows the formation of magnetic polyanions with unprecedented topologies. The magnetic behavior of compounds **1** and **2** have been modeled by using a single $\{J_x, J_y, J_z\}$ exchange parameter set. In contrast, two and four sets of values for the modeling of the magnetic behaviors of complexes **3** and **4**, respectively, are required. For **5**, a simplified model would imply at least three sets of values. It follows that detailed information concerning the magnetic exchange interactions for these systems can be obtained only by combining experimental techniques. As inelastic neutron scattering (INS) spectroscopy has proved to be a valuable tool for the determination of exchange interactions, in particular for the parameters connected with magnetic anisotropy,^[14e, 15b, 16, 35a] such experiments should be performed on compounds **4** and **5**, and the results will be reported elsewhere. Considering that complex **3** is obtained in poor yield and that relatively large amounts of it would be needed for INS measurements, the magnetic study of this compound is not envisaged. The solution studies of compounds **2**, **3**, **4**, and **5**, even if mainly qualitative, led to the conclusion that the structure and the atomic composition seemed to have a strong influence on the voltammetric behaviors of both the W and Co centers. However, the impossibility of studying all the compounds at all pH values excludes a more detailed comparison of the electrochemical behaviors. In the cases of **3** and **4**, the expected electronic effect has been observed. The study of these cobalt compounds in nonaqueous solvents may bring about new insights.

Experimental Section

Chemicals, reagents, and analyses: All chemicals were used as purchased, without purification. The lacunary precursors $Na_{10}[A-\alpha-SiW_9O_{34}]\cdot 19H_2O$ and $K_8[\gamma-SiW_{10}O_{36}]\cdot 12H_2O$ were synthesized as previously described.^[39]

Elemental analysis was performed by the Service Central d'Analyse of the CNRS, 69390 Vernaison (France). Infrared spectra (KBr pellets) were recorded on an IRFT Nicolet 550 apparatus.

K₂₀[(B-β-SiW₉O₃₃(OH))(β-SiW₈O₂₉(OH)₂Co₃(H₂O)₂Co(H₂O)₂]-47H₂O (1**):** $K_8[\gamma-SiW_{10}O_{36}]\cdot 12H_2O$ (0.4 g, 0.13 mmol) and $Co(CH_3COO)_2\cdot 4H_2O$ (0.067 g, 0.27 mmol) were dissolved in water (10 mL). The reaction mixture was stirred at room temperature for 1 h. Then the pH was adjusted to 5 with HCl (0.5 M) and maintained at this value for 15 min. The resulting solution was allowed to evaporate at room temperature; after one week, purple parallelepipedic crystals suitable for X-ray diffraction were filtered and washed with KCl (2 M) solution (yield 0.074 g, 22% based on tungsten). FTIR (KBr pellets): $\tilde{\nu}=987$ (sh), 946 (m), 893 (s), 845 (s), 798

(s), 720 (s), 629 (sh), 534 (w), 490 cm⁻¹ (w); elemental analysis calcd (%) for H₁₁₂Co₇K₂₀O₁₈₃Si₄W₃₄: W 58.98, Co 3.89, K 7.39; found: W 59.30, Co 4.04, K 6.93.

K₇[Co₁₅(H₂O)₇](γ-SiW₁₀O₃₆)(β-SiW₈O₃₀(OH))Co₄(OH)(H₂O)₇·36H₂O (2): After dissolution of K₈[γ-SiW₁₀O₃₆]·12H₂O (0.4 g, 0.13 mmol) and Co(CH₃COO)₂·4H₂O (0.067 g, 0.27 mmol) in water (10 mL), solid potassium cyanate (0.021 g, 0.26 mmol) was added. The reaction mixture was stirred at room temperature for 1 h. Then the pH was adjusted to 5 with HCl (0.5 M) and maintained at this value for 15 min. The resulting solution was allowed to evaporate at room temperature; after one week, purple parallelepipedic crystals suitable for X-ray diffraction were filtered and washed with KCl (2 M) solution (yield 0.12 g, 30% based on tungsten). FTIR (KBr pellets): $\tilde{\nu}$ = 1002 (w), 991 (w), 943 (m), 902 (sh), 869 (s), 792 (s), 773 (m), 557 (w), 528 cm⁻¹ (w); elemental analysis calcd (%) for H₁₀₂Co_{5.5}K₈O₁₁₈Si₂W₁₈: W 55.58, Co 5.44, K 4.60; found: W 55.16, Co 5.58, K 4.68.

K₂Na₃[(A-α-SiW₉O₃₄)Co₄(OH)₃(CH₃COO)₃]·18H₂O (3): Na₁₀[A-α-SiW₉O₃₄]·19H₂O (1 g, 0.35 mmol) and Co(CH₃COO)₂·4H₂O (0.346 g, 1.42 mmol) were dissolved in an aqueous solution of potassium acetate (1 M, 8 mL) adjusted to pH 8 with HCl (1 M). The solution was stirred at 40 °C for 30 min, then cooled to room temperature. The purple suspension was centrifuged to remove insoluble solids, and allowed to evaporate slowly. After one week, purple parallelepipedic crystals suitable for X-ray diffraction were filtered and washed with KCl solution (2 M) (yield 0.095 g, 8% based on tungsten). FTIR (KBr pellets): $\tilde{\nu}$ = 1606 (m), 1556 (m), 1443 (sh), 1421 (s), 1348 (w), 983 (w), 944 (sh), 933 (s), 889 (s), 858 (sh), 808 (s), 742 (w), 674 (s), 539 (m), 523 cm⁻¹ (m); elemental analysis calcd (%) for C₆H₄₈Co₄K₂Na₃O₆₁SiW₉: W 50.45, Co 7.19, K 5.96, Na 2.10, C 2.20; found: W 48.76, Co 7.42, K 5.85, Na 1.50, C 2.01.

K₂Na₃[(A-α-SiW₉O₃₄)Co₄(OH)(N₃)₂(CH₃COO)₃]·18H₂O (4): Na₁₀[A-α-SiW₉O₃₄]·19H₂O (1 g, 0.35 mmol) and Co(SO₄)·7H₂O (0.400 g, 1.42 mmol) were dissolved in an aqueous solution of potassium acetate (0.5 M, 8 mL) adjusted to pH 8 with HCl solution (1 M). Sodium azide (0.140 g, 2.15 mmol) was added and the solution was stirred at 40 °C for 30 min. It was cooled to room temperature, then the purple suspension was centrifuged to remove insoluble solids and allowed to evaporate slowly. After one week, purple parallelepipedic crystals suitable for X-ray diffraction were filtered and washed with KCl solution (2 M) (yield 0.405 g, 34% based on tungsten). FTIR (KBr pellets): $\tilde{\nu}$ = 2098 (s), 1594 (m), 1555 (m), 1437 (m), 1348 (w), 1283 (w), 984 (w), 933 (m), 888 (s), 855 (m), 804 (s), 771 (w), 698 (s), 673 (sh), 524 cm⁻¹ (m); elemental analysis calcd (%) for C₆H₄₆N₆Co₄K₂Na₃O₅₉SiW₉: W 49.69, Co 7.08, K 5.87,

Na 2.07, C 2.16, N 2.52; found: W 45.68, Co 7.43, K 5.74, Na 2.14, C 2.11, N 2.42.

K₈Na₈[(A-α-SiW₉O₃₄)₂Co₈(OH)₆(H₂O)₂(CO₃)₃]·52H₂O (5): Na₁₀[A-α-SiW₉O₃₄]·19H₂O (1 g, 0.35 mmol) and Co(SO₄)·7H₂O (0.400 g, 1.42 mmol) were dissolved in an aqueous solution of sodium acetate (0.5 M, 20 mL) adjusted to pH 8 with HCl (1 M). An aqueous solution of potassium carbonate (2 M, 0.714 mL, 1.42 mmol) was added and the resulting solution was stirred for 1 h at room temperature. The purple suspension was centrifuged to remove insoluble solids and allowed to evaporate slowly. After three days, purple plate-like crystals suitable for X-ray diffraction were filtered and washed with KCl solution (2 M) (yield 0.709 g, 62% based on tungsten). FTIR (KBr pellets): $\tilde{\nu}$ = 1482 (m), 1417 (sh), 1379 (m), 983 (w), 933 (w), 884 (s), 858 (sh), 797 (s), 681 (m), 528 cm⁻¹ (w); elemental analysis calcd (%) for C₃H₁₁₄Co₈K₈Na₈O₁₃₇Si₂W₁₈: W 49.56, Co 7.06, K 4.68, Na 2.75, C 0.54; found: W 47.72, Co 7.44, K 4.85, Na 2.76, C 0.61.

X-ray crystallography: Intensity data were collected with a Siemens SMART three-circle diffractometer for complexes **1**, **2**, and **3** and with a Bruker Nonius X8 Apex 2 diffractometer for complexes **4** and **5**, each equipped with a CCD bidimensional detector using the monochromated wavelength $\lambda(\text{MoK}\alpha) = 0.71073 \text{ \AA}$. All the data were recorded at room temperature except those for complex **4** for which, due to its instability, a single crystal was mounted on a glass fiber in Paratone-N oil and intensity data were collected at 100 K. The absorption correction was based on multiple and symmetry-equivalent reflections in the data set using the SADABS program^[40] based on Blessing's method.^[41] The structures were solved by direct methods and refined by full-matrix least-squares using the SHELX-TL package.^[42] In all the structures there is a discrepancy between the formulae determined by elemental analysis and those deduced from the crystallographic atom list because of the difficulty in locating all the disordered water molecules and alkali counterions. Disordered water molecules, alkali metals, and cobalt counterions were refined with partial occupancy factors. Crystallographic data are given in Table 1. Further details of the crystal structure investigations for **1**, **2**, and **5**, may be obtained from the Fachinformationszentrum Karlsruhe, 76344 Eggenstein-Leopoldshafen, Germany (fax: (+49)7247-808-666; e-mail: crystdata@fiz-karlsruhe.de) on quoting the depository numbers CSD-416950 (**1**), CSD-416951 (**2**), and CSD-416949 (**5**). CCDC-619251 and CCDC-619252 contain the supplementary crystallographic data for compounds **3** and **4**. These data can be obtained free of charge from the Cambridge Crystallographic Data Centre via www.ccdc.cam.ac.uk/data_request/cif.

Table 1. Crystallographic data for complexes **1**–**5**.

	1	2	3	4	5
formula	H ₁₁₂ Co ₇ K ₂₀ O ₁₈₃ Si ₄ W ₃₄	H ₁₀₂ Co _{5.5} K ₇ O ₁₁₈ Si ₂ W ₁₈	C ₆ H ₄₈ Co ₄ K ₂ Na ₃ O ₆₁ SiW ₉	C ₆ H ₄₆ N ₆ Co ₄ K ₂ Na ₃ O ₅₉ SiW ₉	C ₃ H ₁₁₄ Co ₈ K ₈ Na ₈ O ₁₃₇ Si ₂ W ₁₈
<i>M_r</i>	10546.9	5953.9	3279.3	3329.3	6676.3
<i>T</i> [K]	293(2)	293(2)	293(2)	100(2)	293(2)
crystal system	triclinic	triclinic	monoclinic	rhombohedral	triclinic
space group	<i>P</i> $\bar{1}$	<i>P</i> $\bar{1}$	<i>P</i> ₂ / <i>m</i>	<i>R</i> $\bar{3}$	<i>P</i> $\bar{1}$
<i>a</i> [Å]	12.3165(2)	16.8134(5)	10.7959(15)	12.1420(8)	11.9057(2)
<i>b</i> [Å]	17.6051(1)	17.7692(5)	14.803(3)	12.1420(8)	24.2828(5)
<i>c</i> [Å]	19.3340(1)	17.8630(5)	19.137(5)	76.137(7)	41.7373(9)
α [°]	84.858(1)	119.398(1)	90	90	78.452(1)
β [°]	78.032(1)	98.058(1)	93.407(18)	90	89.463(1)
γ [°]	85.501(1)	91.492(1)	90	120	80.751(1)
<i>V</i> [Å ³]	4076.91(7)	4575.7(2)	3053(1)	9721.0(13)	11665.2(4)
<i>Z</i>	2	2	3	6	4
ρ_{calcd} [g cm ⁻³]	3.877	3.994	3.548	3.300	3.488
μ [mm ⁻¹]	24.921	23.950	18.434	17.280	19.190
data/parameters	20308/1107	22615/1198	8256/441	6401/285	66979/2995
<i>R</i> _{int}	0.0540	0.0909	0.0557	0.0362	0.0489
goodness of fit	0.841	0.990	1.034	1.315	1.118
<i>R</i> [<i>I</i> > 2 σ (<i>I</i>)]	<i>R</i> ₁ ^[a] = 0.0816 <i>wR</i> ₂ = 0.1374	<i>R</i> ₁ = 0.0740 <i>wR</i> ₂ = 0.1095	<i>R</i> ₁ = 0.0571 <i>wR</i> ₂ ^[b] = 0.2062	<i>R</i> ₁ = 0.0364 <i>wR</i> ₂ = 0.1700	<i>R</i> ₁ = 0.0412 <i>wR</i> ₂ = 0.1119

$$[a] R_1 = \frac{\sum ||F_o| - |F_c||}{\sum |F_o|} \quad [b] wR_2 = \sqrt{\frac{\sum w(F_o - F_c)^2}{\sum w(F_o)^2}}$$

Magnetic properties: Variable-temperature susceptibility measurements were carried out in the range 2–300 K at a magnetic field of 0.1 T and in the range 2–20 K at a magnetic field of 0.1, 0.5, 1, and 2.5 T on a polycrystalline sample with a magnetometer (Quantum Design MPMS-XL-5) equipped with a SQUID sensor. The susceptibility data were corrected for the diamagnetic contributions using Pascal's constant tables.

UV/Vis spectroscopy: Before the redox properties of polyoxometalates were studied, it was necessary to determine their stability domains over the pH scale being used. It is known that polyanions may undergo chemical transformations or decompose completely, depending on the pH of the solution in which they are dissolved. For the stability tests, UV/Vis spectra of polyoxometalate-containing solutions recorded as a function of time were compared. All solutions were 2×10^{-5} M in polyanion and were placed in quartz cuvettes with an optical path of 1 cm. Spectra were recorded with a Lambda 19 Perkin-Elmer spectrophotometer.

Electrochemical experiments: Ultrapure water was used, obtained by successive purification cycles in a Millipore RiOS 8 system, followed by passage through a Milli-Q Academic module. All chemicals were reagent grade of commercial origin. Pure NO (N20 grade) was purchased from Air Liquide, France. NO was introduced into an oxygen-free electrochemical cell through a catheter connected to a sealed purging system previously filled with argon which excluded oxygen and allowed contaminants such as NO_x to be scavenged in KOH (9M). NO was bubbled through the electrolyte in the electrochemical cell for 30 min, resulting in an NO-saturated solution (1–2 mM). The electrochemical cell was checked for leaks by keeping solutions saturated with NO for several hours and using them for electrocatalytic reduction of this substrate; after chasing NO by bubbling pure argon in, no electroactivity of NO or a related species could be detected in the potential range from +0.8 V to –0.8 V at pH 0.33.

The composition and pH of the media used in this work, both in the electrochemical experiments and in the stability studies by spectrophotometry, were: 0.5 M H₂SO₄, pH 0.33; 0.4 M CH₃COONa + ClCH₂COOH, pH 3; 0.4 M CH₃COONa + CH₃COOH, pH 5; 0.4 M NaH₂PO₄ + NaOH, pH 6 and pH 7.

For all compounds, the polyanion concentration was 2×10^{-4} M, unless otherwise indicated. The solutions were de-aerated thoroughly for at least 30 min with pure argon and kept under a positive pressure of Ar during the experiments. The source, mounting, and polishing of the glassy carbon (GC, Tokai, Japan) electrodes has been described.^[43] The glassy carbon samples had a diameter of 3 mm. The electrochemical setup was an EG&G 273A potentiostat/galvanostat driven by a PC with the EG&G M270 software. Potentials were measured versus a saturated calomel electrode (SCE). The counter electrode was a platinum gauze of large surface area. All experiments were performed at room temperature.

Acknowledgements

This work was supported by the CNRS (UMR 8180 and UMR 8000), the University Paris-Sud XI, the University of Versailles-Saint-Quentin and the Spanish Ministerio de Educación y Cultura (CTQ2005-09385-C03-01/PPQ).

- [1] G. Hervé, A. Tézé, R. Contant, in *Polyoxometalate Molecular Science* (Eds.: J. J. Borrás-Almenar, E. Coronado, A. Müller, M. T. Pope), Kluwer Academic, Dordrecht (The Netherlands), **2003**, p. 33.
- [2] M. T. Pope, *Heteropoly and Isopoly Oxometalates*, Springer, Berlin (Germany), **1983**.
- [3] J. M. Clemente-Juan, E. Coronado, *Coord. Chem. Rev.* **1999**, *193–195*, 361.
- [4] a) I. V. Kozhevnikov, *Catalysis by Polyoxometalates*, Wiley, Chichester (UK), **2002**; b) N. Mizuno, N. Misono, *Chem. Rev.* **1998**, *98*, 199; c) R. Neumann, *Prog. Inorg. Chem.* **1998**, *47*, 317; d) C. L. Hill, C. M. Prosser-McCarthy, *Coord. Chem. Rev.* **1995**, *143*, 407.

- [5] Throughout the text, the term nuclearity refers to the number of neighboring paramagnetic centers.
- [6] S. S. Mal, U. Kortz, *Angew. Chem.* **2005**, *117*, 3843; *Angew. Chem. Int. Ed.* **2005**, *44*, 3777.
- [7] B. Godin, Y.-G. Chen, J. Vaissermann, L. Ruhlmann, M. Verdaguer, P. Gouzerh, *Angew. Chem.* **2005**, *117*, 3132; *Angew. Chem. Int. Ed.* **2005**, *44*, 3072.
- [8] P. Mialane, A. Dolbecq, J. Marrot, E. Rivière, F. Sécheresse, *Angew. Chem.* **2003**, *115*, 3647; *Angew. Chem. Int. Ed.* **2003**, *42*, 3523.
- [9] P. Mialane, A. Dolbecq, F. Sécheresse, *Chem. Commun.* **2006**, 3477.
- [10] P. Mialane, A. Dolbecq, J. Marrot, E. Rivière, F. Sécheresse, *Chem. Eur. J.* **2005**, *11*, 1771.
- [11] P. Mialane, C. Duboc, J. Marrot, E. Rivière, A. Dolbecq, F. Sécheresse, *Chem. Eur. J.* **2006**, *12*, 1950.
- [12] P. Mialane, A. Dolbecq, E. Rivière, J. Marrot, F. Sécheresse, *Angew. Chem.* **2004**, *116*, 2324; *Angew. Chem. Int. Ed.* **2004**, *43*, 2274.
- [13] a) L. C. W. Baker, T. P. McCutcheon, *J. Am. Chem. Soc.* **1956**, *78*, 4503; b) H. Andres, M. Aebersold, H. U. Güdel, J. M. Clemente-Juan, E. Coronado, H. Büttner, D. Kearley, M. Zolliker, *Chem. Phys. Lett.* **1998**, *289*, 224.
- [14] a) T. J. R. Weakley, H. T. Evans, Jr., J. S. Showell, G. F. Tourné, C. M. Tourné, *J. Chem. Soc. Chem. Commun.* **1973**, 139; b) R. G. Finke, M. W. Droegge, P. J. Domaille, *Inorg. Chem.* **1987**, *26*, 3886; c) L.-H. Bi, E.-B. Wang, J. Peng, R.-D. Huang, L. Xu, C.-W. Hu, *Inorg. Chem.* **2000**, *39*, 671; d) L.-H. Bi, R.-D. Huang, J. Peng, E.-B. Wang, Y.-H. Wang, C.-W. Hu, *J. Chem. Soc. Dalton Trans.* **2001**, 121; e) H. Andres, J. M. Clemente-Juan, M. Aebersold, H. U. Güdel, E. Coronado, H. Büttner, G. Kearly, J. Melero, R. Burriel, *J. Am. Chem. Soc.* **1999**, *121*, 10028; f) J. M. Clemente-Juan, H. Andres, M. Aebersold, J. J. Borrás-Almenar, E. Coronado, H. U. Güdel, H. Büttner, G. Kearly, *Inorg. Chem.* **1997**, *36*, 2244; g) N. Casañ-Pastor, J. Bas-Serra, E. Coronado, G. Pourroy, L. C. W. Baker, *J. Am. Chem. Soc.* **1992**, *114*, 10380; h) M. Clemente-León, E. Coronado, J.-R. Galán-Mascarús, C. Giménez-Saiz, C. J. Gómez-García, T. Fernández-Otero, *J. Mater. Chem.* **1998**, *8*, 309; i) C. J. Gómez-García, E. Coronado, J. J. Borrás-Almenar, *Inorg. Chem.* **1992**, *31*, 1667.
- [15] a) C. M. Tourné, G. F. Tourné, F. Zonnevillje, *J. Chem. Soc. Dalton Trans.* **1991**, 143; b) J. M. Clemente-Juan, E. Coronado, A. Gaita-Ariño, C. Giménez-Saiz, G. Chaboussant, H.-U. Güdel, R. Burriel, H. Mutka, *Chem. Eur. J.* **2002**, *8*, 5701; c) L. Ruhlmann, J. Canny, R. Contant, R. Thouvenot, *Inorg. Chem.* **2002**, *41*, 3811; d) J. M. Clemente-Juan, E. Coronado, A. Gaita-Ariño, C. Giménez-Saiz, H.-U. Güdel, R. Sieber, R. Bircher, H. Mutka, *Inorg. Chem.* **2005**, *44*, 3389.
- [16] H. Andres, J. M. Clemente-Juan, R. Basler, M. Aebersold, H.-U. Güdel, J. J. Borrás-Almenar, A. Gaita-Ariño, E. Coronado, H. Büttner, S. Janssen, *Inorg. Chem.* **2001**, *40*, 1943.
- [17] M. D. Ritorto, T. M. Anderson, W. A. Neiwert, C. L. Hill, *Inorg. Chem.* **2004**, *43*, 44.
- [18] J. M. Clemente-Juan, E. Coronado, A. Forment-Aliaga, J.-R. Galán-Mascarús, C. Giménez-Saiz, C. J. Gómez-García, *Inorg. Chem.* **2004**, *43*, 2689.
- [19] a) T. J. R. Weakley, *J. Chem. Soc. Chem. Commun.* **1984**, 1406; b) J.-R. Galán-Mascarús, C. J. Gómez-García, J. J. Borrás-Almenar, E. Coronado, *Adv. Mater.* **1994**, *6*, 221.
- [20] B. S. Bassil, U. Kortz, A. S. Tigan, J. M. Clemente-Juan, B. Keita, P. de Oliveira, L. Nadjo, *Inorg. Chem.* **2005**, *44*, 9360.
- [21] B. S. Bassil, S. Nellutla, U. Kortz, A. C. Stowe, J. van Tol, N. S. Dalal, B. Keita, L. Nadjo, *Inorg. Chem.* **2005**, *44*, 2659.
- [22] Elemental analysis calcd (%) for H₉₄Co₃K₁₄O₁₁₅Si₂W₁₈: W 54.93, Co 2.94, K 9.09; found: W 54.86, Co 3.25, K 9.08.
- [23] N. M. Okun, T. M. Anderson, C. L. Hill, *J. Am. Chem. Soc.* **2003**, *125*, 3194.
- [24] K. Nakamoto, *Infrared and Raman Spectra of Inorganic and Coordination Compounds*, Wiley, New York (USA), **1997**.
- [25] G. B. Deacon, R. J. Phillips, *Coord. Chem. Rev.* **1980**, *33*, 227.
- [26] There is an uncertainty about the Δ_1 value for compound **3** and the Δ_2 value for compound **4** as the band at 1440 cm⁻¹ appears as a

- shoulder at 1421 cm^{-1} for **3** and the band at 1417 cm^{-1} appears as a shoulder at 1437 cm^{-1} for **4**; these values can be estimated to $\pm 5\text{ cm}^{-1}$.
- [27] a) R. Cortes, J. I. R. Delarramendi, L. Lezama, T. Rojo, K. Urtiaga, M. I. Arriortua, *J. Chem. Soc. Dalton Trans.* **1992**, 2971; b) M. G. Barandika, R. Cortes, L. Lezama, K. Urtiaga, M. I. Arriortua, T. Rojo, *J. Chem. Soc. Dalton Trans.* **1999**, 2971.
- [28] B. M. Gatehouse, S. E. Livingstone, R. S. Nyholm, *J. Chem. Soc.* **1958**, 3137.
- [29] N. E. Brese, M. O'Keeffe, *Acta Crystallogr. Sect. B* **1991**, 47, 192.
- [30] A. J. Gaunt, I. May, D. Collison, O. D. Fox, *Inorg. Chem.* **2003**, 42, 5049.
- [31] Z. Zhang, Y. Li, E. Wang, X. Wang, C. Qin, H. An, *Inorg. Chem.* **2006**, 45, 4313.
- [32] a) K. Wassermann, H.-J. Lunk, R. Palm, J. Fuchs, N. Steinfeldt, R. Stösser, M. T. Pope, *Inorg. Chem.* **1996**, 35, 3273; b) X. Wei, M. H. Dickman, M. T. Pope, *Inorg. Chem.* **1997**, 36, 130; c) U. Kortz, *J. Cluster Sci.* **2003**, 14, 205; d) P. Mialane, A. Dolbecq, E. Rivière, J. Marrot, F. Sécheresse, *Eur. J. Inorg. Chem.* **2004**, 33.
- [33] U. Kortz, A. Tézé, G. Hervé, *Inorg. Chem.* **1999**, 38, 2038.
- [34] a) F. Meyer, P. Rutsch, *Chem. Commun.* **1998**, 1037; b) B. Kersting, *Angew. Chem.* **2001**, 113, 4109; *Angew. Chem. Int. Ed.* **2001**, 40, 3987; c) J. Glerup, K. Michelsen, N. Arulsamy, D. J. Hodgson, *Inorg. Chim. Acta* **1998**, 274, 155.
- [35] a) J. J. Borrás-Almenar, J. M. Clemente-Juan, E. Coronado, B. S. Tsukerblat, *Inorg. Chem.* **1999**, 38, 6081; b) J. J. Borrás-Almenar, J. M. Clemente-Juan, E. Coronado, B. S. Tsukerblat, *J. Comput. Chem.* **2001**, 22, 985.
- [36] $R = [\sum(\chi_M T_{\text{calc}} - \chi_M T_{\text{obs}})^2 / \sum(\chi_M T_{\text{obs}})^2]$.
- [37] a) E. Papaconstantinou, M. T. Pope, *Inorg. Chem.* **1967**, 6, 1152; b) R. Contant, J. M. Fruchart, *Rev. Chim. Minérale* **1974**, 11, 123; c) B. Keita, Y. W. Lu, L. Nadjo, R. Contant, *Electrochem. Commun.* **2000**, 2, 720.
- [38] a) I. M. Mbomekalle, B. Keita, M. Nierlich, U. Kortz, P. Berthet, L. Nadjo, *Inorg. Chem.* **2003**, 42, 5143; b) D. Jabbour, B. Keita, I. M. Mbomekalle, L. Nadjo, U. Kortz, *Eur. J. Inorg. Chem.* **2004**, 2036.
- [39] A. Tézé, G. Hervé, *Inorg. Synth.* **1990**, 27, 85.
- [40] G. M. Sheldrick, SADABS, Program for Scaling and Correction of Area Detector Data, University of Göttingen, Göttingen (Germany), **1997**.
- [41] R. Blessing, *Acta Crystallogr. Sect. A* **1995**, A51, 33.
- [42] G. M. Sheldrick, SHELX-TL, Version 5.03, Software Package for Crystal Structure Determination, Siemens Analytical X-ray Instrument Division, Madison, WI (USA), **1994**.
- [43] B. Keita, F. Girard, L. Nadjo, R. Contant, J. Canny, M. Richet, *J. Electroanal. Chem.* **1999**, 478, 76.

Received: September 1, 2006
Published online: January 17, 2007